Quantitative Super-Resolution Microscopy

Harkes, R.

CHAPTER 4

DIRECT OBSERVATION OF α-SYNUCLEIN AMYLOID AGGREGATES[1]

Abstract

Aggregation of α-synuclein has been linked to both familial and sporadic Parkinson's disease. Recent studies suggest that α-synuclein aggregates may spread from cell to cell and raise questions about the propagation of neurodegeneration. While continuing progress has been made characterizing α-synuclein aggregates *in vitro*, there is a lack of information regarding structure of these species inside the cells. Here, we use confocal fluorescence microscopy in combination with super-resolution microscopy to investigate α-synuclein uptake when added exogenously to SH-SY5Y neuroblastoma cells, and to probe *in situ* morphological features of α-synuclein aggregates with near nanometer resolution. We were able to follow the uptake of α-synuclein aggregates by the cells and their partial degradation at a molecular level. Our data show that the cellular uptake via endocytosis is rapid. Once the aggregates are internalized, they accumulate in lysosomes where they are degraded. No further aggregation was observed inside the lysosomes as speculated in literature, nor in the cytoplasm of the cells. These results show the importance of the lysosome-dependent mechanism for protecting the cells from exposure to potentially toxic α-synuclein.

[1]This chapter is based on: Mihaela M. Apetri, Rolf Harkes, Vinod Subramaniam, Gerard W. Canters, Thomas Schmidt and Thijs J. Aartsma, Direct observation of α-synuclein amyloid aggregates in endocytic vesicles of neuroblastoma cells
Submitted to FEBS letters

4.1 INTRODUCTION

Progressive accumulation and deposition of specific protein aggregates is a characteristic of many neurodegenerative disorders, including Parkinson's disease (PD). In PD, α-synuclein(α-syn), a small presynaptic protein (~ 15 kDa), is the main fibrillar component of the intraneuronal protein aggregates (Lewy bodies) that represent the pathological feature of this disease[1]. Although α-syn is predominantly a cytosolic protein, recent studies suggest the protein exerts not only a pathogenic effect inside the cells, but an extracellular pathogenic action as well. Multiple forms of α-syn have been observed in cerebrospinal fluid, blood plasma and more recently, in saliva[2–4]. When applied to cultured cells, α-syn preformed aggregates are internalized via endocytosis and targeted to the lysosomes for degradation[5–9]. The extent of aggregate accumulation inside cells is determined by the cells ability to degrade and remove the aggregates. Few groups reported that α-syn take-up from the extracellular space induces the aggregation of the endogenous protein, leading to the formation of Lewy body-like inclusions[9–12]. Cell to cell transmission of α-syn pathological aggregates has been demonstrated in neuronal cultured cells as well as in animal models[13,14]. They show this is most likely through sequential exocytosis and endocytosis.

At this moment, the fate of the exogeneous α-syn aggregates once they enter the cells is not clear. Are the aggregates degraded in the lysosomes, or do they start growing into larger α-syn aggregates? Do they overload the degradation systems impairing their activity and escape in the cytosol inducing aggregation of the endogeneous protein? In order to address these questions, we followed directly the uptake and fate of α-syn preformed aggregates when added to neuroblastoma cells, SH-SY5Y, by super-resolution microscopy.

While atomic force microscopy (AFM) has been extensively used to obtain the ultrastructure and morphological features of the amyloid aggregates, the technique has the drawback to be applicable only *ex situ*. In contrast, optical microscopy and in particular the new super-resolution methods are powerful and non-invasive techniques for the study of morphological features of the amyloid aggregates with nanometer resolution. In the last years, these optical techniques have been successfully used in several studies to probe the morphology of protein aggregates *in vitro*[15–17] and in cells[18–20].

Here we applied confocal fluorescence microscopy and optical super-resolution microscopy to follow and characterize the fate of small *in vitro* assembled α-syn

fibrils in human neuroblastoma cells. We found that fibrils were partially degraded when trafficked through the lysosomal pathway. Further fibril maturation and formation of long fibrils was not observed. Our study thus highlights the potential role of lysosomal degradation in the prevention of α-syn aggregation in cells.

4.2 MATERIALS AND METHODS

4.2.1 Preparation of labeled α-syn fibrillar seeds

Recombinant human wild type α-syn was expressed and purified as described previously[21]. Fibrils were formed at 37 ºC in 1.5 ml Eppendorf tubes under constant agitation (1000 rpm, in an Eppendorf Thermomixer comfort, Eppendorf AG, Germany). 300 μL of 70 μM α-syn in phosphate buffer saline (PBS) was incubated for 5 days. The presence of amyloid fibrils was confirmed by thioflavin T fluorimetry and atomic force microscopy. Labeling of α-syn fibrils with the NHS ester (succinimidyl ester) of Alexa Fluor 532 was performed according to the manufacturer's instructions (Life Technologies, USA). Briefly, α-syn fibril solution was incubated for 1 h at room temperature with Alexa Fluor 532 dye in a 1:1 protein/ fluorophore molar ratio. The unbound dye was removed by pelleting the fibrils at 13000 rpm for 15 min in a tabletop centrifuge. The supernatant was discarded and the pellet containing labeled fibrils was resuspended in PBS. The centrifugation/resuspension cycle was repeated twice. Purified labeled α-syn fibrils were divided in 20 μL aliquots, flash frozen and stored at -80 ºC. Fibrillar seeds of α-syn were produced as follows: 20 μL of labeled fibrils were diluted 10 times in PBS and sonicated 3×5 s with a probe sonicator (Sonics & Materials, Inc., USA) using 50% maximum power, yielding variable fibril lengths of approximately 350 nm. These seeds were added immediately in the culture medium of SH-SY5Y cells at a final concentration of 100 nM, and their uptake by the cells was followed in time using confocal microscopy and direct stochastic optical reconstruction microscopy (dSTORM).

4.2.2 Cell culture

Human neuroblastoma cells, SH-SY5Y, (gift of Mireille M. A. E. Claessens, University of Twente, Netherlands) were grown in 1:1 minimum essential media (MEM) (Gibco by Life Technologies, USA) and nutrient mixture Ham's F-12 (PAN Biotech, Germany) free of phenol red, supplemented with 1% MEM, non-essential amino acids, 2mM Glutamax and 15% fetal bovine serum (Gibco by Life Technologies).

4.2.3 Atomic force microscopy (AFM)

Labeled α-syn fibrillar samples were diluted 5 times into PBS, and 10 μL were pipetted onto freshly cleaved mica and kept at room temperature for 60 s. The mica surface was then rinsed with Millipore-filtered water (2×50 μL) to remove loosely bound protein, dried under a stream of nitrogen and imaged immediately.

AFM imaging was performed on a MultiMode Nanoscope IIIa microscope (Digital Instruments, USA) equipped with an E-scanner. All measurements were carried out in the tapping mode under ambient conditions using single-beam silicon cantilever probes with a resonant frequency of 300 kHz (Olympus, Japan). Image analysis was performed using the instrument software.

4.2.4 Co-localization experiments with lysosomes

SH-SY5Y cells were incubated with 50 nM LysoTracker® Deep Red (Life Technologies) for 30 min at 37 ºC, then washed and incubated further with 100 nM Alexa532-labeled α-syn sonicated fibrils. Cells were imaged live after α-syn seeds addition, using an adapted confocal spinning-disk setup based on an Axiovert 200 body microscope (Zeiss, Germany) with a spinning disk confocal unit (CSU-X1 Yokogawa, Japan) and a back-illuminated EMCCD camera (iXON 897, Andor, UK) on the side port. The temperature was kept at 37 ºC with constant 5% CO_2 concentration in a stage-top incubator (Tokai Hit, Japan). Illumination was performed with two different lasers of wavelength 514 nm (Cobolt, Sweden) and 642 nm (Spectra-Physics, USA).

4.2.5 dSTORM experiments and data analysis

In vitro prepared α-syn fibrils, labeled with Alexa 532, were spin coated onto a glass coverslip in 1% poly vinyl alcohol (Sigma Aldrich) and imaged. Imaging was performed in a switching buffer solution: 100 mM mercaptoethylamine (Sigma Aldrich) in PBS (pH 8.0) [22]. On day before imaging, SH-SY5Y were plated at 10^5 cells on 35 mm ibidi treated glass bottom dishes (ibidi GmbH, Germany) and then incubated with 100 nM final concentration of α-syn seeds labeled with Alexa 532. Cells were fixed in 4% formaldehyde at different incubation times and then imaged in the switching buffer.

dSTORM set-up

Super-resolution imaging was performed on a home-built wide-field single molecule setup, based on an Axiovert S100 Zeiss inverted wide-field microscope equipped with a 100x 1.4 NA oil-immersion objective (Zeiss, Germany). The Alexa 532 dye was excited using a 532 nm laser (Cobolt, Sweden). A 405 nm laser (CrystaLaser, USA) was used for photo-switching and to adjust the density of visible fluorophores. The light was reflected into the objective by the dichroic mirror ZT405/532/635rpc (Chroma, USA). The fluorescence light in the detection path was filtered using the emission filter ZET532/633m (Chroma, USA). Conversion intensities were in between 0 and 20 W/cm^2 at 405 nm and

the excitation intensity was 3 kW/cm^2 at 532 nm. For each sample, we acquired 10000 single molecule images with an acquisition time of 10 ms per frame and a frame rate of 87 Hz. The signal of individual dye molecules was captured on a sCMOS Orca Flash 4.0V2 camera (Hamamatsu, Japan) (Fig.1a). The average integrated signal of a single dye molecule was 447 detected photons (Fig.1d), spatially distributed by the 2 dimensional point-spread-function of the microscope of 293 nm FWHM (Fig.1c).

Data analysis

The signal from individual fluorophores (Fig.1c) was fitted with a 2 dimensional Gaussian using a custom least-squares algorithm in Matlab[23]. From the fit we determined the location of each molecule to high accuracy of 11 nm on average (Fig.1b). The localization accuracy coincides with the value predicted from the width of the point-spread-function and the detected number of photons, 293 nm / $\sqrt{[447]}$ = 14 nm. Subsequently, the localization data were used to generate super-resolution images. Super-resolution images were obtained by binning localizations into 20x20 nm^2 bins. For zoom-ins we used probability density maps in which each localization was represented as a normalized Gaussian centered at the position and of width given by the sigma-uncertainty in localization. The pixel size was chosen to represent 1x1 nm^2.

For analysis of fiber width and length we used line fitting from the raw localization data. We selected a region of interest (ROI) around a fibril. The selected localizations were rotated and subsequently the y-coordinates of the localizations were binned. The full width at half-maximum (FWHM) was calculated from the resulting histogram (see supplemental Fig.S1). Given that localizations in dSTORM experiments had an average positional accuracy of 11 nm (Fig.1b), leading to an apparent FWHM of $11\times2\sqrt{[2\times\log(2)]}$=26 nm for any point object. The apparent FWHM of the fiber was therefore de-convolved to give the true fiber width, $FWHM_d = \sqrt{[FWHM^2-(26\text{ nm})^2]}$.

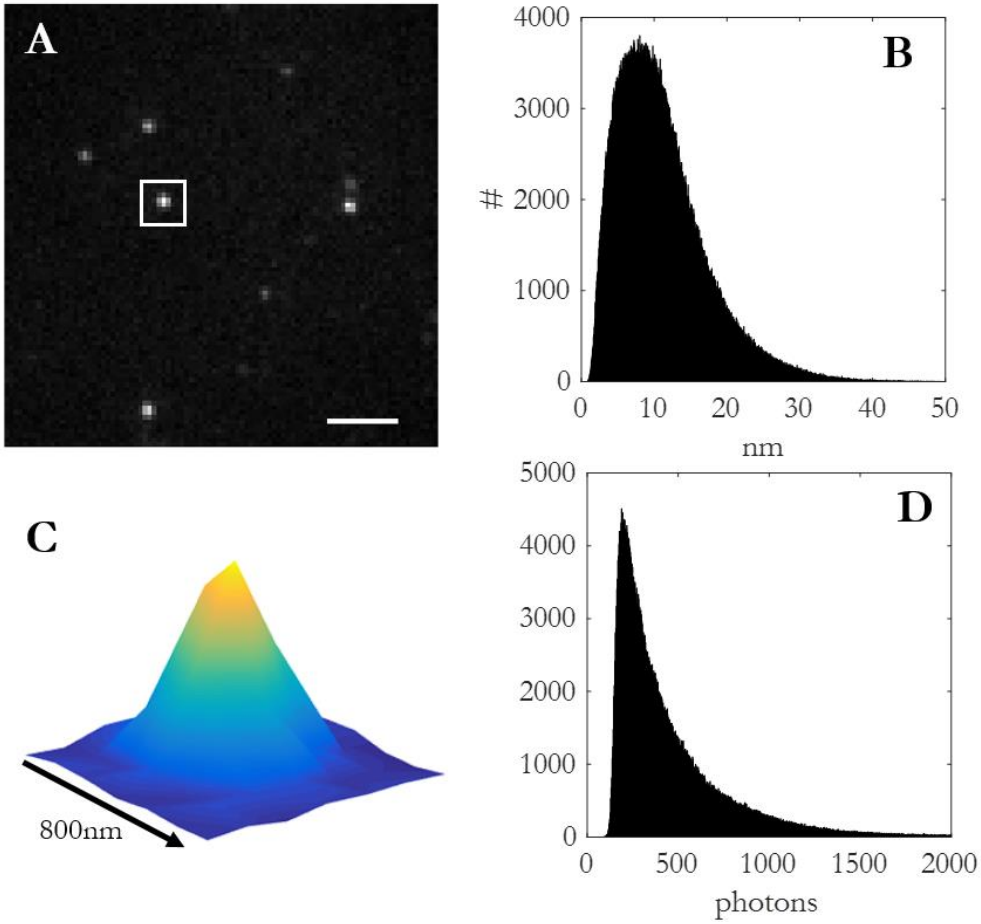

Figure 1: Characteristic properties of the optical setup. (a) Frame with the signal of several Alexa532 molecules. Scale bar = 2µm. (b) Histogram of the sigma of positional accuracy (Mean: 11 nm). (c) Zoom-in of the white square in figure 1a showing the Gaussian intensity profile. (d) Histogram of the intensity of localizations (Mean: 447 photons).

4.3 RESULTS AND DISCUSSION

4.3.1 Super-resolution imaging of *in vitro* α-syn fibrils

In this study we used direct stochastic reconstruction microscopy (dSTORM) to follow the uptake of α-syn aggregates by SH-SY5Y human neuroblastoma cells. dSTORM has been used in several studies to probe the morphology of protein aggregates such as Aβ-aggregates in Alzheimer's disease[18,19], Huntington's protein aggregates in Huntington's disease[15,24] and α-syn amyloid fibrils in Parkinson's disease (PD) [16]. In relation to earlier studies, we here used direct fluorescence labeling of α-syn by switchable fluorophores. Direct labeling is advantageous when compared to other superresolution methods which typically involve immunofluorescence labeling, the latter leading to substantial increase in structure size due to the antibody size (~10 nm) as compared to the small size of fluorescent dyes used in the current study.

We first characterized the properties of α-syn amyloid *in vitro* fibrils prepared in our conditions. Figure 2 shows the morphology of labeled intact α-syn fibrils as obtained by AFM (Fig. 2a) and by dSTORM (Fig. 2b) when deposited at low concentration onto a flat substrate. Individual fibrils were clearly identified in both methods. The overall images appear very comparable. The length of the fibrils clearly exceeded 1 μm extending to 10 μm and longer. In view of the complex topology of the fibrous network with fiber crossings, a detailed statistical analysis of fiber length was omitted.

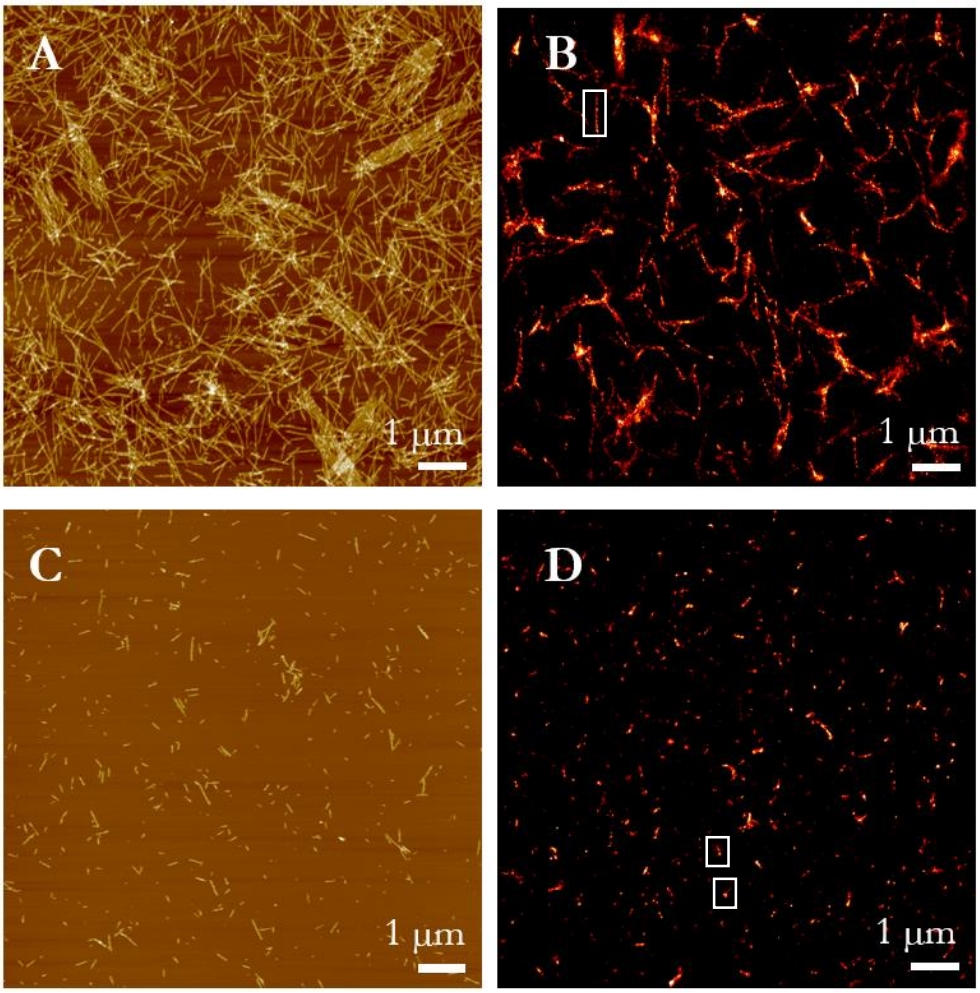

Figure 2: Super-resolution imaging of the in vitro prepared α-syn fibrils. (a) AFM and (b) dSTORM images of intact wild-type α-syn fibrils covalently labeled with the NHS derivate of Alexa 532 fluorophore. (c) AFM and (d) dSTORM images of sonicated labeled α-syn fibrils.

The apparent width of the fibers was determined from the dSTORM images as detailed in the materials and methods sub-section. A zoom-in of the fibril marked in figure 2b is shown in figure 3a. From the histogram of localizations (Fig. 3b) the apparent width of the fiber was 47nm FWHM (dashed red line). The distribution of apparent widths for 38 fibrils is shown in figure 3c. The distribution is characterized by a mean of FWHM = 43 ± 12 nm. Deconvolution leads to the real fiber widths of 34 ± 12 nm. This result by optical microscopy was compared to results by AFM experiments. In AFM experiments, we used

the height information to estimate the diameter of the labeled α-syn fibrils. The height approach is generally assumed more accurate than measurements of the width as of tip-convolution[25]. The mean height was found to be 8 ± 1 nm for the labeled α-syn fibrils (mean ± s.e. from 50 fibers, see supplemental Fig.S2). The apparent discrepancy in fiber widths between the two methods seems not too surprising. It is well known that AFM underestimates heights of nanometer size objects such as proteins[26], due to sample deformation and/or dehydration.

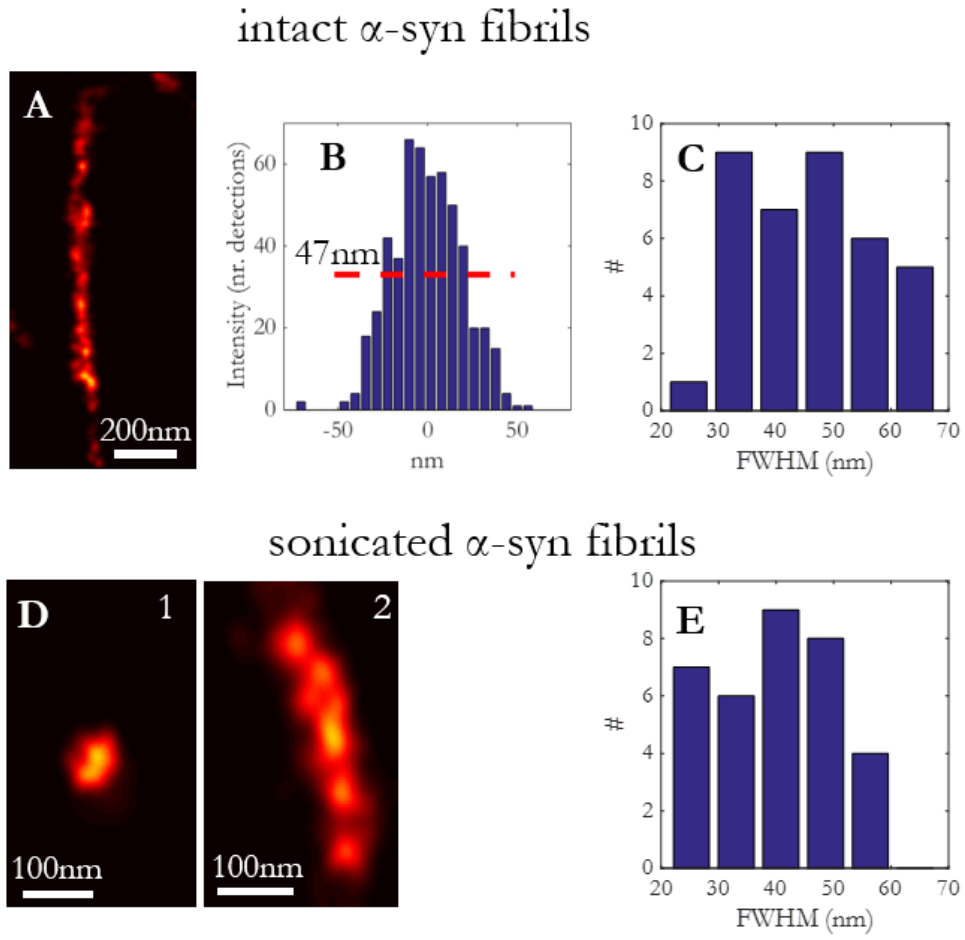

Figure 3: Characterization of different sized a-syn fibrils by dSTORM. (a) Detailed view of an intact a-syn - Alexa532 fibril (the marked fibril from figure 2b). (b) Histogram corresponding to the localization data (see supplementary figure 1 for details on the method). A FWHM of 47nm was calculated. (c) Histogram distribution of FWHM for intact α-syn fibrils. A mean diameter of 43.4 ± 12.3 nm was calculated from FWHM data (> 25 fibrils). (d) dSTORM images of two different sized sonicated fibrils (the marked

sonicated fibrils from figure 2d). (e) Histogram distribution of FWHM for sonicated α-syn fibrils. The mean diameter of α-syn sonicated fibrils was 42 ± 11 nm.

α-Syn aggregates have been reported to be internalized into a variety of cell types, including neurons[7,9,12]. It has been shown that the uptake is more efficient if the aggregates are smaller. For this reason, α-syn fibrils were sonicated prior to their addition to the cells. The effect of sonication on fibril size is already apparent in Figure 2. Whereas fibril length clearly exceeds 1 μm for the intact fibrils (Fig. 2a&b), after sonication the length shortened to <1 μm (Fig. 2c&d) independent of the imaging method used. The lengths of the sonicated fibrils determined by AFM were between 50 and 700 nm. The lengths determined by dSTORM were similar, and in the range between 30 and 650 nm. The smaller length fibrils appear as globular (Fig. 3d 1) whereas the longer structures as clear fibrils (Fig. 3d 2). While sonication led to a significant decrease in fibril length, the fibril width was unchanged. The distribution of sonicated fibril width, as shown in Figure 3e, is characterized by a mean of 42 ± 11 nm, which leads, after deconvolution, to a real width of $FWHM_d$ of 32 ± 11 nm.

4.3.2 Internalization of extracellular α-syn fibrils into neuronal cells

Having established that we were able to distinguish small sized α-syn aggregates *in vitro*, we moved further to study the fate of the aggregates once they are exogenously added to cells in culture. We investigated the uptake of the small fibrillar α-syn aggregates labeled with Alexa-532 dye by the SH-SY5Y human neuroblastoma cells using confocal fluorescence microscopy.

The time-course of uptake is seen in figure 4. Sonicated, labeled seeds were added at a concentration of 100 nM to the culture medium and left during the experiment. Their uptake by SH-SY5Y cells was followed in time using confocal microscopy and dSTORM. In the first 2 hours α-syn aggregates were mostly present at the cell membrane resulting in images that resemble typical images of the cell's outline (Fig. 4 left&middle). After 24 hours Alexa532-syn aggregates disappear from the outer cell membrane and localize as granular intracellular deposits mostly close to the nucleus (Fig. 4 right). This observation suggests that fibrils were internalized and probably processed in the endosomal pathway towards perinuclear lysosomes. This interpretation is supported by dual color experiments which showed that the granular deposits (Fig. 4 green) colocalized with a marker for acidic organelles, such as lysosomes (LysoTracker; Fig. 4 red). Hence, our data confirm earlier results which suggested that protein aggregates

like α-syn are transported towards the lysosomal compartment for degradation and clearance[6,7].

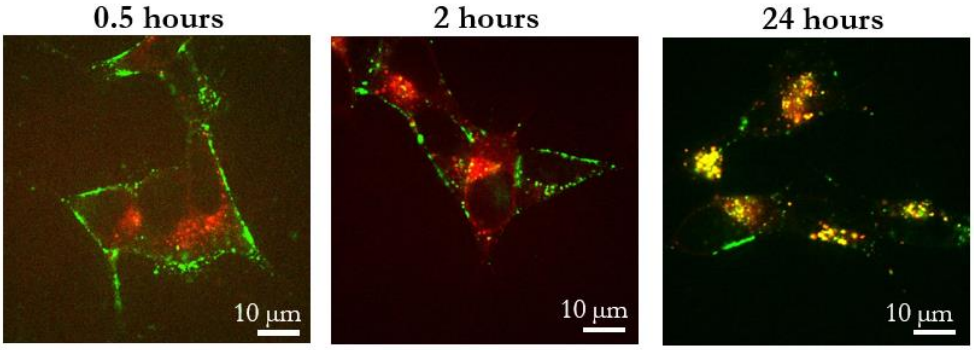

Figure 4: Internalization of α-syn sonicated fibrils in human neuroblastoma cells. Images show co-localization of Alexa 532 labeled α-syn aggregates (green) with the lysosomes labeled with LysoTracker® Deep Red (red). SH-SY5Y cells were treated with 50nM LysoTracker® Deep Red, then washed, incubated further with Alexa532-labeled α-syn sonicated fibrils and imaged live on a confocal microscope.

Subsequently we addressed whether maturation and increase in aggregation of fibrils occurred while transported from the plasma membrane to the endosomes/lysosomes. Whether and how maturation occurs and whether that will lead to some equilibrium distribution of aggregates, monomers and degraded peptide in cells when being continuously exposed to an extracellular concentration is still unclear. One proposed mechanism for maturation, that has been linked to disease, is that fibrils further aggregate inside the acidic endocytic vesicles as the combination of low pH and high effective concentration are favorable conditions for α-syn aggregation[27]. Further it is unclear whether such maturation would lead to the formation of long α-syn fibrils in the cytoplasm of the cells.

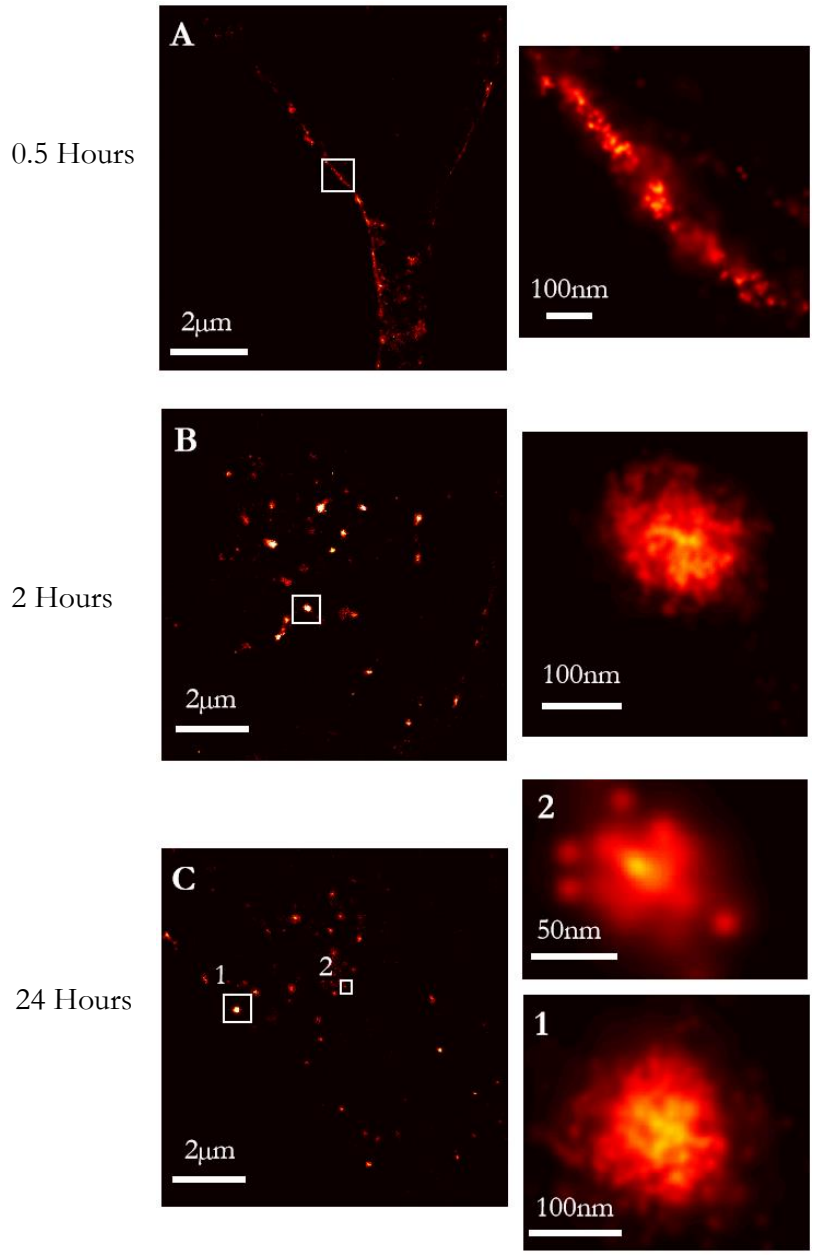

Figure 5: Super-resolution images of internalized α-syn aggregates in endosomal vesicles in time. a) dSTORM image of a cell treated for half an hour with α-syn-Alexa532 aggregates. A detailed view of the aggregates in the cell membrane is shown in the image to the right. (b) After 2 hours of incubation, α-syn aggregates are internalized in vesicles. Detailed view of the aggregates in a vesicle shown in the image to the right b). (c) Internalized α-syn aggregates after 24 hours of incubation, with two different sized clusters shown to the right.

To address these questions, we used the super-resolution capability of dSTORM to probe directly the morphology of α-syn aggregates while entering SH-SY5Y cells (Fig.5). The dSTORM images, like the confocal images in figure 4, showed that α-syn aggregates initially associated with, and accumulated at the plasma membrane (Fig.5a). In the course of time cells took up the fibrils and accumulated them in endocytic vesicles (Fig.5b&c). Inside the vesicles the aggregates appeared tightly packed forming bigger clusters. The typical size of those intracellular globular structures stretched from 30 - 150 nm. It is worth mentioning that the small-sized fibrils did not completely lose their morphology even after 72 hours (Fig.5b&c). Endosomes and lysosomes are typically 50–400 nm in diameter and are distributed uniformly throughout the cytosol[28]. Hence, the size of the clusters, as determined by live-cell dSTORM, falls into the small size region expected for endosomes and lysosomes.

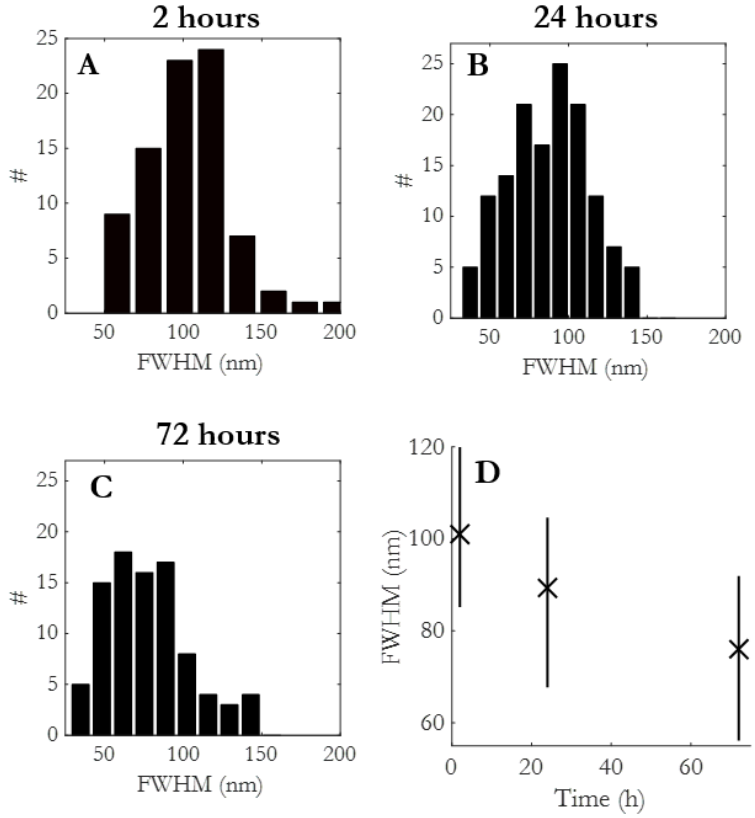

Figure 6: Size distribution of α-syn aggregates in endosomal vesicles in time. (a)-(c) Histogram distribution of intracellular α-syn clusters FWHM in time. (d) A clear decrease in α-syn cluster size is observed in the representation of the mean average FWHM of α-syn clusters in time (x = median - = 50% interval).

The size of the clusters appeared to decrease as proteins moved through the endosomal pathway towards lysosomes (Fig.6). The size decreased from 104 ± 32 nm at 2 h after incubation to 78 ± 28 nm after 72 h. This significant decrease might be interpreted as onset of lysosomal breakdown. It should be stressed that we did not observe maturation and formation of α-syn fibrils in the cytoplasm over a period of 3 days. This is a clear difference from our (see Fig.2) and others *in vitro* results in which long (> 1 μm) fibrils were already formed within this time span. It is important to note that, with the exception of Lewy bodies[9,29] there is so-far no clear evidence for the presence of linear α-syn amyloid fibrils within mammalian cells. Hence, our data further refutes the model in which fibril maturation proceeds within the cells and finally will lead to disease in Parkinson's.

In conclusion, our study provides additional evidence in favor of a lysosomal degradation pathway for removal of extracellular α-syn aggregates. Cells internalize extracellular small sized fibrils (<1 μm length). Subsequently the aggregates accumulate in endocytic vesicles and are trafficked towards lysosomes. Fibrils keep their morphology and do not further mature but rather partially degrade as they move through endosomal pathway. As lysosomal malfunction has been linked to neurodegeneration and age-related neurodegenerative disorders[30,31], enhancing lysosomal function may be a potential therapeutic strategy for prevention or treatment of PD. Since our study did not focus on the effect of longer (>1 μm) fibers on cellular processes and cell viability, their potential impact of long fibers in disease should not be overlooked.

Acknowledgments

We thank Dr. Mireille M. A. E. Claessens at University of Twente for kindly providing a human neuroblastoma cell line, SH-SY5Y and Nathalie Schilderink for expressing and purifying human wild type α-syn. This work is part of the research program 'Single Molecule Point of View in Aggregation' of the Foundation for Fundamental Research on Matter (FOM), which is part of the Netherlands Organization for Scientific Research (NWO).

4.4 REFERENCES

[1] M. G. Spillantini, M. L. Schmidt, V. M. Lee, J. Q. Trojanowski, R. Jakes, and M. Goedert, Nature 388, 839 (1997).

[2] R. Borghi, R. Marchese, A. Negro, L. Marinelli, G. Forloni, D. Zaccheo, G. Abbruzzese, and M. Tabaton, Neurosci. Lett. 287, 65 (2000).

[3] I. Devic, H. Hwang, J. S. Edgar, K. Izutsu, R. Presland, C. Pan, D. R. Goodlett, Y. Wang, J. Armaly, V. Tumas, C. P. Zabetian, J. B. Leverenz, M. Shi, and J. Zhang, Brain 134, e178 (2011).

[4] O. M. El-Agnaf, S. A. Salem, K. E. Paleologou, M. D. Curran, M. J. Gibson, J. A. Court, M. G. Schlossmacher, and D. Allsop, FASEB J. 20, 419 (2006).

[5] D. Freeman, R. Cedillos, S. Choyke, Z. Lukic, K. McGuire, S. Marvin, A. M. Burrage, S. Sudholt, A. Rana, C. O'Connor, C. M. Wiethoff, and E. M. Campbell, PLoS ONE 8, e62143 (2013).

[6] H.-J. J. Lee, F. Khoshaghideh, S. Patel, and S.-J. J. Lee, J. Neurosci. 24, 1888 (2004).

[7] H.-J. J. Lee, J.-E. E. Suk, E.-J. J. Bae, J.-H. H. Lee, S. R. Paik, and S.-J. J. Lee, Int. J. Biochem. Cell Biol. 40, 1835 (2008).

[8] J. Y. Sung, J. Kim, S. R. Paik, J. H. Park, Y. S. Ahn, and K. C. Chung, J. Biol. Chem. 276, 27441 (2001).

[9] L. A. Volpicelli-Daley, K. C. Luk, T. P. Patel, S. A. Tanik, D. M. Riddle, A. Stieber, D. F. Meaney, J. Q. Trojanowski, and V. M. Lee, Neuron 72, 57 (2011).

[10] K. M. Danzer, S. K. Krebs, M. Wolff, G. Birk, and B. Hengerer, J. Neurochem. 111, 192 (2009).

[11] K. C. Luk, C. Song, P. O'Brien, A. Stieber, J. R. Branch, K. R. Brunden, J. Q. Trojanowski, and V. M. Lee, Proc. Natl. Acad. Sci. U.S.A. 106, 20051 (2009).

[12] L. A. Volpicelli-Daley, K. C. Luk, and V. M. Lee, Nat Protoc 9, 2135 (2014).

[13] P. Desplats, H.-J. J. Lee, E.-J. J. Bae, C. Patrick, E. Rockenstein, L. Crews, B. Spencer, E. Masliah, and S.-J. J. Lee, Proc. Natl. Acad. Sci. U.S.A. 106, 13010 (2009).

[14] C. Hansen, E. Angot, A.-L. L. Bergström, J. A. Steiner, L. Pieri, G. Paul, T. F. Outeiro, R. Melki, P. Kallunki, K. Fog, J.-Y. Y. Li, and P. Brundin, J. Clin. Invest. 121, 715 (2011).

[15] W. C. Duim, B. Chen, J. Frydman, and W. E. Moerner, Chemphyschem 12, 2387 (2011).

[16] D. Pinotsi, A. K. Buell, C. Galvagnion, C. M. Dobson, G. S. Kaminski Schierle, and C. F. Kaminski, Nano Lett. 14, 339 (2014).

[17] J. Ries, V. Udayar, A. Soragni, S. Hornemann, K. P. Nilsson, R. Riek, C. Hock, H. Ewers, A. A. Aguzzi, and L. Rajendran, ACS Chem Neurosci 4, 1057 (2013).

[18] E. K. Esbjörner, F. Chan, E. Rees, M. Erdelyi, L. M. Luheshi, C. W. Bertoncini, C. F. Kaminski, C. M. Dobson, and G. S. Kaminski Schierle, Chem. Biol. 21, 732 (2014).

[19] G. S. Kaminski Schierle, S. van de Linde, M. Erdelyi, E. K. Esbjörner, T. Klein, E. Rees, C. W. Bertoncini, C. M. Dobson, M. Sauer, and C. F. Kaminski, J. Am. Chem. Soc. 133, 12902 (2011).
[20] M. J. Roberti, J. Fölling, M. S. Celej, M. Bossi, T. M. Jovin, and E. A. Jares-Erijman, Biophys. J. 102, 1598 (2012).
[21] A. Sidhu, I. Segers-Nolten, and V. Subramaniam, Biochim. Biophys. Acta 1844, 2127 (2014).
[22] M. Heilemann, S. van de Linde, A. Mukherjee, and M. Sauer, Angew. Chem. Int. Ed. Engl. 48, 6903 (2009).
[23] T. Schmidt, G. J. Schütz, W. Baumgartner, H. J. Gruber, and H. Schindler, Proc. Natl. Acad. Sci. U.S.A. 93, 2926 (1996).
[24] S. J. Sahl, L. E. Weiss, W. C. Duim, J. Frydman, and W. E. Moerner, Sci Rep 2, 895 (2012).
[25] C. Bustamante and D. Keller, Phys. Today 48, 32 (1995).
[26] M. E. Fuentes-Perez, M. S. Dillingham, and F. Moreno-Herrero, Methods 60, 113 (2013).
[27] V. N. Uversky and D. Eliezer, Curr. Protein Pept. Sci. 10, 483 (2009).
[28] R. A. Nixon and A. M. Cataldo, Trends Neurosci. 18, 489 (1995).
[29] R. A. Crowther, S. E. Daniel, and M. Goedert, Neurosci. Lett. 292, 128 (2000).
[30] B. A. Bahr and J. Bendiske, J. Neurochem. 83, 481 (2002).
[31] R. A. Nixon, A. M. Cataldo, and P. M. Mathews, Neurochem. Res. 25, 1161 (2000).

4.5 SUPPLEMENTARY FIGURES

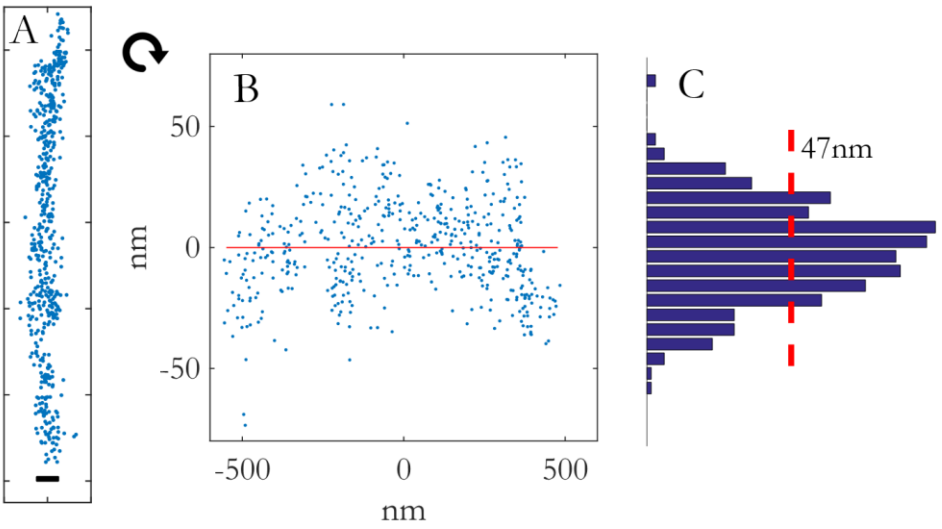

Figure S1: FWHM determination. (a) The 526 localizations of the single fibril from figure 3a. Scale bar = 50nm (b) Locations are rotated so the angle of a linear fit is 0 (red line). (c) Y-coordinates are binned into $\sqrt{N}$ bins. FWHM is determined from linear interpolation of the histogram to be 47nm. (red dashed line)

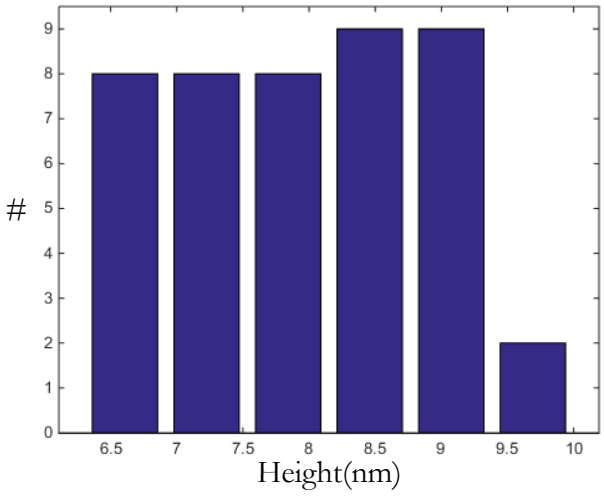

Figure S2: Height distribution of fibrils obtained by AFM.